Fault-Tolerant Control of Electric Vehicles with In-Wheel Motors through Tyre-Force Allocation

Daniel Wanner[1*], Johannes Edrén[1], Mats Jonasson[1,2], Oskar Wallmark[3], Lars Drugge[1], Annika Stensson Trigell[1]

[1]KTH Royal Institute of Technology, School of Engineering Science, Department of Aeronautical and Vehicle Engineering, Stockholm, Sweden
[2]Vehicle Dynamics and Active Safety, Volvo Car Corporation, Gothenburg, Sweden
[3]KTH Royal Institute of Technology, School of Electrical Engineering, Laboratory of Electrical Energy Conversion, Stockholm, Sweden

Teknikringen 8
SE-100 44 Stockholm, SWEDEN
Phone: +46 8 790 7805

E-mail: dwanner@kth.se

This paper presents a fault handling strategy for electric vehicles with in-wheel motors. The applied control algorithm is based on tyre-force allocation. One complex tyre-force allocation method, which requires non-linear optimization, as well as a simpler tyre force allocation method are developed and applied. A comparison between them is conducted and evaluated against a standard reference vehicle with an Electronic Stability Control (ESC) algorithm. The faults in consideration are electrical faults that can arise in in-wheel motors of permanent-magnet type. The results show for both tyre-force allocation methods an improved re-allocation after a severe fault and thus results in an improved state trajectory recovery. Thereby the proposed fault handling strategy becomes an important component to improve system dependability and secure vehicle safety.

Topics / Fault-Tolerant Control, Force Allocation, Integrated Chassis Control

1. INTRODUCTION

Vehicles with electric drivetrains and by-wire chassis systems provide potential improvements in terms of passenger safety, comfort and handling [1, 2]. With an increased level of electrification, the number of ways on how to influence the vehicle movement can also be increased; an electric machine can be used for providing tractive as well as braking forces. This leads to a higher level of functional integration applying combined forces in longitudinal, lateral, and vertical direction with each actuator. Different studies have shown that electric vehicles with over-actuation have the capability to increase vehicle safety by applying tyre-force allocation techniques [3–7]. A wheel unit can be formed on each wheel that controls the longitudinal, lateral and vertical corner forces [8]. However, an increased level of electrification also increases the amount of possible failure modes that can occur during operation [9]. Studies with real over-actuated vehicles on fault accommodation have been conducted by [10]. As a result, further research in this area is necessary and in several surveys it is recommended to further improve system dependability [11].

This study focuses on longitudinal directed over-actuation deploying four in-wheel motors. Different tyre-force allocation control methods are compared with each other as well as to a standard electronic stability control system. One allocation method is a simplified algebraic algorithm, which is qualified for online application, while the other method is an optimization approach. A typical fault for in-wheel motors is induced during cornering. The performance and limitations of the different control methods are compared.

2. ELECTRIC VEHICLE SPECIFICATIONS

The studied vehicle represents a typical compact passenger car with an all-electric drive train (see Fig. 1). The mass of the vehicle includes a 200 kg battery pack which is mounted in the body floor. This leads to a changed weight distribution compared to a conventional vehicle. In addition to the standard components of the chassis such as friction brakes, passive steering and passive suspension system, each of the four wheels accommodate an in-wheel motor with a planetary gear transmission. Four separate inverters control the flow of power from and to each motor. A lithium-ion battery pack and a super capacitor deliver the power requested through the inverters to the in-wheel motors. The

in-wheel motors are assumed to be permanent magnet synchronous machines (PMSM) with an outer-rotor design specifically designed for vehicle aspects, such as certain speed-torque curve, reduced torque ripple and light-weight characteristics. Each PMSM can deliver a continuous power of 15 kW with rated torque of 180 Nm at a driving speed of 70 km/h. The faster charge and discharge characteristics of the supercapacitor, connected to the DC-link via a DC/DC-converter, enables a transient buffer for fast power transfer that compensates the limitations of the battery pack.

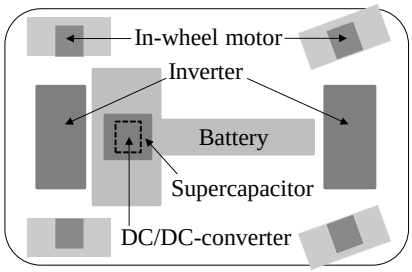

Fig. 1. Vehicle configuration.

The vehicle configuration is shown in Fig. 1, while the vehicle parameters are described in Table 1.

Table 1. Vehicle parameters.

Body mass	m	1460 kg
In-wheel motor mass	m_{em}	17.5 kg
Body roll moment of inertia	I_{xx}	542 kgm^2
Body pitch moment of inertia	I_{yy}	2480 kgm^2
Body yaw moment of inertia	I_{zz}	2656 kgm^2
CoG to front axle distance	l_f	1.08 m
CoG to rear axle distance	l_r	1.57 m
Front track width	s_f	1.54 m
Rear track width	s_r	1.53 m
CoG to ground height	h	0.54 m
Dynamic tyre roll radius	r_{dyn}	0.30 m
Front spring stiffness	c_1, c_2	33000 N/m
Rear spring stiffness	c_3, c_4	56000 N/m
Front anti roll-bar stiffness	c_{12}	20006 N/m
Rear anti roll-bar stiffness	c_{34}	16088 N/m
Front damper coefficient	d_1, d_2	1288 Ns/m
Rear damper coefficient	d_3, d_4	1276 Ns/m
Longitudinal tyre stiffness	C_s	70000 N/rad
Front cornering stiffness	C_1, C_2	25000 N/rad
Rear cornering stiffness	C_3, C_4	40000 N/rad

3. VEHICLE DYNAMICS MODEL

The in-wheel motor driven vehicle is modelled as a two-track model (Fig. 2) with six degrees of freedom, governing longitudinal v_x, lateral v_y, vertical v_z and rotational speeds of the vehicle. The latter are described by pitch $\dot{\theta}$, roll $\dot{\varphi}$ and yaw $\dot{\psi}$ dynamics.

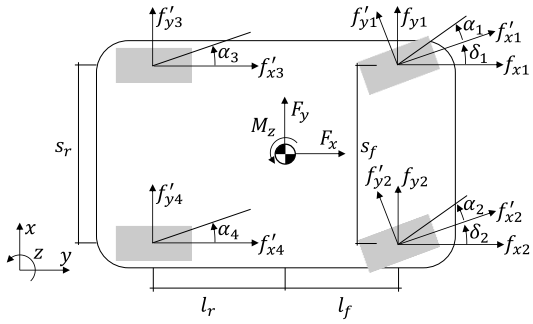

Fig. 2. Vehicle dynamics model.

The tyre model is a simple combined slip model. The longitudinal force $\acute{f}_{x,i}$ consists of a linear longitudinal stiffness and the saturation at the maximum utilization level

$$\acute{f}_{x,i} = \begin{cases} C_s \kappa_i & \acute{f}_{x,i} < \mu_i f_{z,i} \\ \mu_i f_{z,i} & \acute{f}_{x,i} \geq \mu_i f_{z,i} \end{cases} \quad (1)$$

with the longitudinal tyre stiffness C_s, the longitudinal slip κ_i, the friction coefficient μ_i and the vertical load $f_{z,i}$, where the wheel is defined as $i = 1, \ldots, 4$. The lateral force $\acute{f}_{y0,i}$ is given by

$$\acute{f}_{y0,i} = C_i \tan \alpha_i \quad (2)$$

with α_i as the slip angle as well as C_i as the cornering stiffness. The friction circle constrains the maximum applicable lateral force $\acute{f}_{y,i}$ with

$$\acute{f}_{y,i} = \acute{f}_{y0,i} \sqrt{1 - \left(\frac{\acute{f}_{x,i}}{\mu_i f_{z,i}} \right)^2} \quad (3)$$

4. CHARACTERISTICS OF ELECTRIC FAULTS

Electrical faults in an electric machine of permanent magnet type can be characterized by different properties. Especially at high vehicle speed when reaching the field-weakening range, faults in this machine type distinguish from faults in conventional induction machines. In a non-fault condition, the voltage generated by the rotating rotor magnets is countered by the electromagnetic field induced by the inverter.

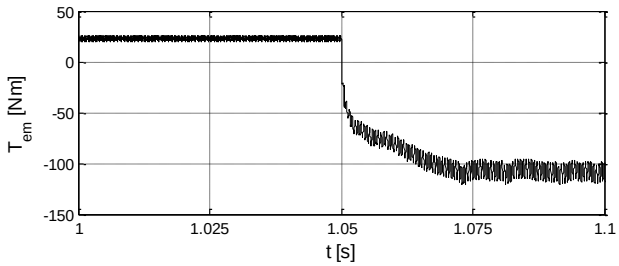

Fig. 3. Torque behaviour for inverter shut-down fault.

A fault analysis was conducted in [12] to specify the severity of different faults. Based on the conclusions

from [12], an inverter shutdown was selected as a representative severe fault for this study. In case of an inverter shut-down fault ay high speeds, a continuous brake torque is generated and the vehicle stability is directly threatened. The torque characteristics with the induction of such a fault after 1.05 s are shown in Fig. 3.

5. CONTROL ARCHITECTURE

The vehicle is chosen to be controlled by the principle of control allocation, which here means that the control task is divided into a closed-loop dynamic motion controller followed by static force allocation controller as seen in Fig. 4. The principle of force allocation has recently got more attention within the research community as well as industry due to the new possibilities with the electrification of drive train and chassis systems [3-8].

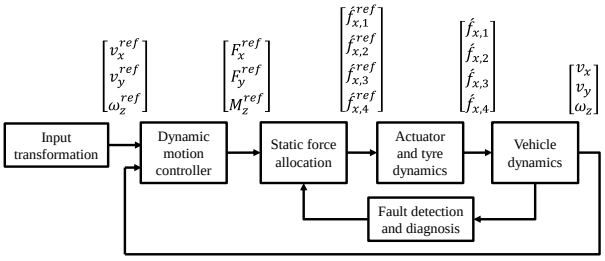

Fig. 4. Structure of the closed-loop vehicle controller.

The pre-set constant reference parameters are vehicle speed v_x^{ref} and curvature R as the input to the simulation model. These values are transformed to lateral velocity v_y^{ref} and yaw velocity ω_z^{ref} with the well-known bicycle model. These reference speeds (v_x^{ref}, v_y^{ref}, ω_z^{ref}) are the inputs to the dynamic motion controller and are compared instantaneously to the measured speeds (v_x, v_y, ω_z) in order to minimise the tracking error. The outputs from the dynamic motion controller are the reference vehicle forces (F_x^{ref}, F_y^{ref}, M_z^{ref}), which represent the longitudinal and lateral force on, and the yaw torque around, the centre of gravity.

The control structure has been augmented with a fault detection and diagnosis function (FDD). This function detects and diagnoses faults and provides the resulting information to the static force allocator in order to re-allocate reference forces to the in-wheel motors in an optimal way. Moreover, it provides isolation of the faulted actuator. Without FDD, the force constraints in the force allocation process might be violated, and as a potential consequence, vehicle safety becomes threatened. Here, it is assumed that the fault detection and diagnosis system [2, 14] is working correctly and complete information about the analysed type of fault is available instantly after its occurrence.

The allocation of the vehicle forces to the in-wheel motors is a mathematically under determined problem, since the number of controlled actuators is higher than the number of degrees of freedom. Non-linear constraints, such as the friction circle, are set to achieve valid solutions. The static force allocation distributes reference tyre forces $\acute{f}_x^{ref} = \left[\acute{f}_{x1}^{ref} \;\; \acute{f}_{x2}^{ref} \;\; \acute{f}_{x3}^{ref} \;\; \acute{f}_{x4}^{ref}\right]^T$ among the four in-wheel motors. Two different types of static force allocators have been studied in this work, referred to as the optimisation approach and the simplified approach.

The least square *optimization approach* allocates the vehicle forces to the tyre forces by minimising the static allocation error. This error is defined as the offset between the reference vehicle forces $F_{veh}^{ref} = \left[F_x^{ref} \;\; F_y^{ref} \;\; M_z^{ref}\right]^T$, and the longitudinal and lateral corner forces, which are defined in the vector $u^{ref} = [\acute{f}_{x1}, \acute{f}_{y1}, \dots, \acute{f}_{y4}]$ that are valid within the tyre force constraints. The general relation is given as

$$F_{veh}^{ref} = BTu^{ref} \tag{5}$$

with the tyre-to-corner transformation matrix T and the geometry matrix

$$\mathrm{B} = \begin{bmatrix} 1 & 0 & 1 & 0 & 1 & 0 & 1 & 0 \\ 0 & 1 & 0 & 1 & 0 & 1 & 0 & 1 \\ -\frac{\mathrm{s_f}}{2} & \mathrm{l_f} & \frac{\mathrm{s_f}}{2} & \mathrm{l_f} & -\frac{\mathrm{s_r}}{2} & -\mathrm{l_r} & \frac{\mathrm{s_r}}{2} & -\mathrm{l_r} \end{bmatrix} \tag{6}$$

where $s_{f,r}$ and $l_{f,r}$ are the track widths for front and rear and the distances from the centre of gravity to the front and rear axle respectively.

The minimisation problem is described as

$$\min \mathrm{g(u)} = \min_{\mathrm{u}} \tfrac{1}{2}\left(\left\|WBTu^{ref} - WF_{veh}^{ref}\right\|_2^2 - \epsilon\|u\|_2^2\right) \tag{4}$$

where $W = \mathrm{diag}(w_1, w_2, w_3)$ is a weighting matrix and ϵ a weight to avoid excessive actuation when it is not needed. The friction ellipse, determining the tyre force constraints, is used for limiting the maximum combined directional forces on each tyre and is derived from the wheel loads as well as the maximum lateral forces that are both inputs into the allocator. Actuator constraints are also taken into account by limiting the propelling torques of the electric machines. The braking torque limitations of the electric machines are supported by friction brakes while decelerating. A complete description of the optimisation approach is described in [14].

The optimisation approach holds a considerable computational burden when it is used on-board in a real vehicle. Hence, a simplified rule-based force allocator has also been applied in the *simplified approach*. Since this allocator does not require any on-board optimization the run time effort is significantly smaller, facilitating an on-board application. The applied algorithm is the Moore-Penrose pseudo-inverse control allocation method, which gives back the minimal L_2 solution of tyre forces and allocates F_x and M_z only. The equations for the pseudo-inverse method are described by the applicable desired forces of each in-wheel motor in the longitudinal direction of the tyre and the uncontrolled

forces in the lateral direction of the tyres. Hence the general relation between vehicle forces $F_{veh}^{ref} = \left[F_x^{ref} \;\; M_z^{ref} \;\; 0\right]^T$, and directional tyre forces $\acute{f}_x^{ref}$ and $\acute{f}_y^{ref} = \left[\acute{f}_{y1}^{ref} \;\; \acute{f}_{y2}^{ref} \;\; \acute{f}_{y3}^{ref} \;\; \acute{f}_{y4}^{ref}\right]^T$ is given by

$$F_{veh}^{ref} = \acute{A}\acute{f}_y^{ref} + \acute{B}\acute{f}_x^{ref} \tag{7}$$

with the longitudinal tyre matrix

$$\acute{B} = \begin{bmatrix} \cos\delta_1 & \cos\delta_2 & 1 & 1 \\ -\frac{s_f\cos\delta_1}{2} + l_f\sin\delta_1 & -\frac{s_r\cos\delta_2}{2} + l_f\sin\delta_2 & -\frac{s_r}{2} & \frac{s_r}{2} \\ k_{f,1} & k_{f,2} & k_{f,3} & k_{f,4} \end{bmatrix} \tag{8}$$

and the lateral tyre matrix

$$\acute{A} = \begin{bmatrix} -\sin\delta_1 & -\sin\delta_2 & 0 & 0 \\ \frac{s_f\sin\delta_1}{2} + l_f\cos\delta_1 & -\frac{s_f\sin\delta_2}{2} + l_f\cos\delta_2 & -l_r & -l_r \end{bmatrix} \tag{9}$$

where δ_i is the steering angle. Assuming that lateral tyre forces $\acute{f}_y^{ref}$ cannot be controlled with the in-wheel motors, the longitudinal tyre forces $\acute{f}_x^{ref}$ are found by calculating the pseudo-inverse of the non-invertible $\acute{B}$-matrix according to

$$\acute{B}^{\dagger} = \acute{B}^T\left(\acute{B}\acute{B}^T\right)^{-1} \tag{10}$$

Then the reference wheel motor torques are governed by

$$T_W^{ref} = r_{dyn}^{-1}\acute{B}^{\dagger}F_{veh}^{ref} \tag{11}$$

The third row in F_{veh}^{ref} sets the longitudinal force for the faulted wheel to zero. The same row in matrix $\acute{B}$ defines the location of the faulty wheel with a fault identifier for each of the i-wheels

$$k_{f,i} = \begin{cases} 0 & non-faulted\ wheel \\ 1 & faulted\ wheel \end{cases} \tag{12}$$

where i represents also the column of the matrix. Thus the applied matrix $\acute{B}^{\dagger}$ is dynamically changing with the fault identifier. In case no fault occurs, i.e. before the fault happens, the $\acute{B}$-matrix is switched to a matrix without the fault identifier row and the zero value in the reference vehicle force vector is omitted. One drawback of this method is that it cannot handle constraints, i.e. when reaching the tyre force constraints or the torque limit of the actuator, the algorithm still allocates torque to the wheels exceeding the limitations. In addition, this method allocates wheel-torques to the wheels independently of normal loads, which means that friction utilisation among the tyres can vary a lot during longitudinal and lateral load transfer.

A simple Electronic Stability Control (ESC) serves as reference for both allocation approaches. This controller applies a braking force on the i-th wheel to achieve a yaw rate error reduction. After exceeding a yaw rate error threshold, the following rule is applied to determine the desired wheel to brake

$$\acute{f}_{x,i}^{ESC} = \acute{f}(\Delta\dot{\psi}, sign(M_z)) \tag{13}$$

where $\Delta\dot{\psi}$ is the difference between the desired and actual yaw rate and $\mathrm{sign}(\mathrm{M_z})$ defines the type of course deviation.

6. RESULTS

A simulation is conducted with the vehicle model described in Section 3 and the control algorithms proposed in Section 4. In order to have a performance reference even for the ESC algorithm, a completely uncontrolled vehicle is plotted as well. The driving scenario selected in this work is a typical high speed steady-state cornering manoeuvre with a curvature of $R = 225\,m$. The steering wheel angle which is calculated from the curvature and a given vehicle speed of $v_x = 33.3\,m/s$ are the reference parameters describing the desired path of the vehicle. The inverter shut-down fault is induced after one second simulation time. The path plots for the different control strategies are shown in Fig. 5.

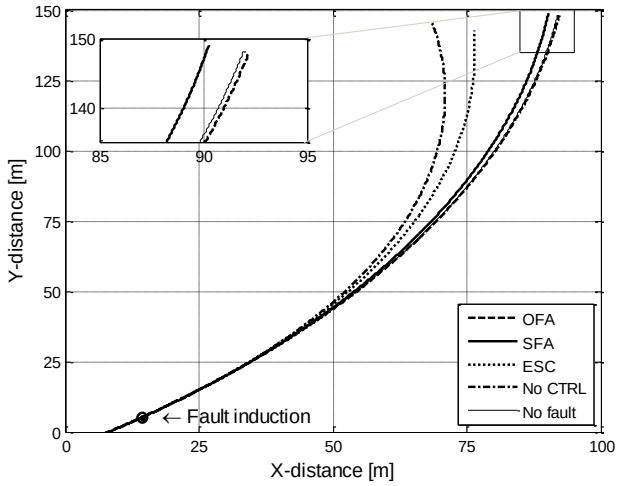

Fig. 5. Path plot for different control strategies; OFA - optimal force allocation; SFA – simple force allocation; ESC – electronic stability control; No CTRL – uncontrolled vehicle; No fault – CFA path without fault.

As the reference path is changing with the vehicle speed (thus varies for different control strategies), the absolute deviation between the path with and without induced fault for every control strategy is shown in Fig. 6. After 4 s of fault induction, the optimisation allocation approach shows very small deviation from its reference path, followed by the simplified allocation with a deviation of less than 1 m. The deviation of the ESC strategy is about 4 m, while the uncontrolled vehicle has a deviation of 6 m.

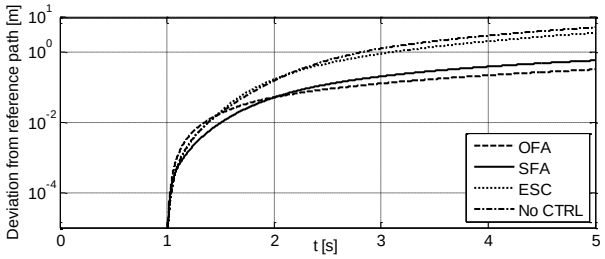

Fig. 6. Overall deviations from reference path for the analysed control strategies.

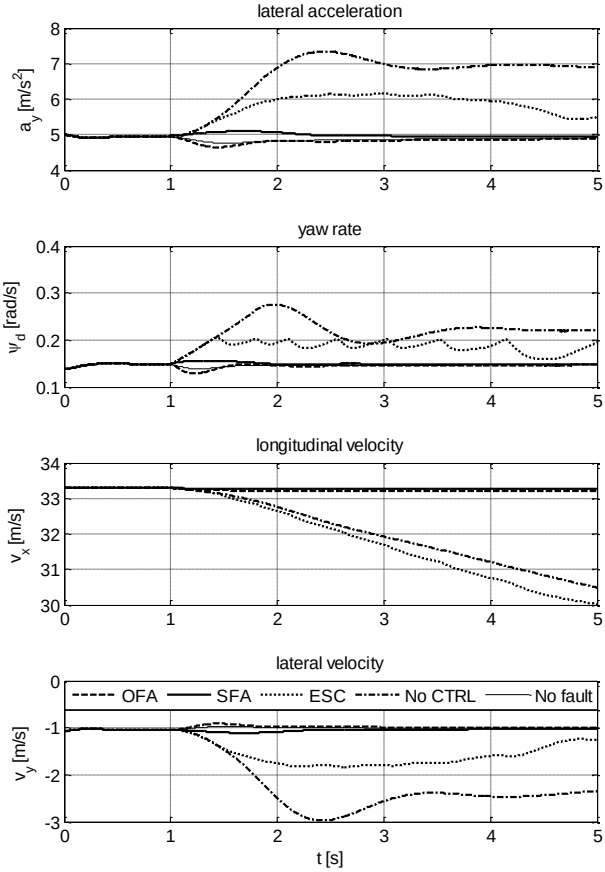

Fig. 7. Vehicle responses with an inverter-shutdown after $t = 1$ s.

The vehicle responses show a distinct difference between the allocation approaches and the reference vehicle with and without ESC. When applying the two different control allocation approaches, all motions are kept at about the same level and very small deviations are visible. Both approaches are reacting quicker and with a lower torque fluctuation, which increases the safety margin of the vehicle. The faulty braking torque on the inner rear wheel is counteracted by a higher positive wheel torque on the inner front wheel. Vehicle speed and the desired trajectory are almost sustained after the fault occurs.

The vehicle with ESC and especially the uncontrolled vehicle results in higher deviations from the original responses. The reference vehicle with ESC counteracts the fault in its typical pulsating way from the intermittent brake actuation, as seen in the yaw rate plot in Fig. 7 and the actual wheel torque plot in Fig. 8. The working principle of applying the outer front brake to induce a counteracting yaw torque is a crucial distinction to the allocation methods. This results in an undesired deceleration of the vehicle speed, which leads to an increase of lateral acceleration and thus to a minor friction reserve and can ultimately cause a rear-end collision. However, a reduction of speed can also be beneficial to decrease the under-steered behaviour and keep a narrow curvature.

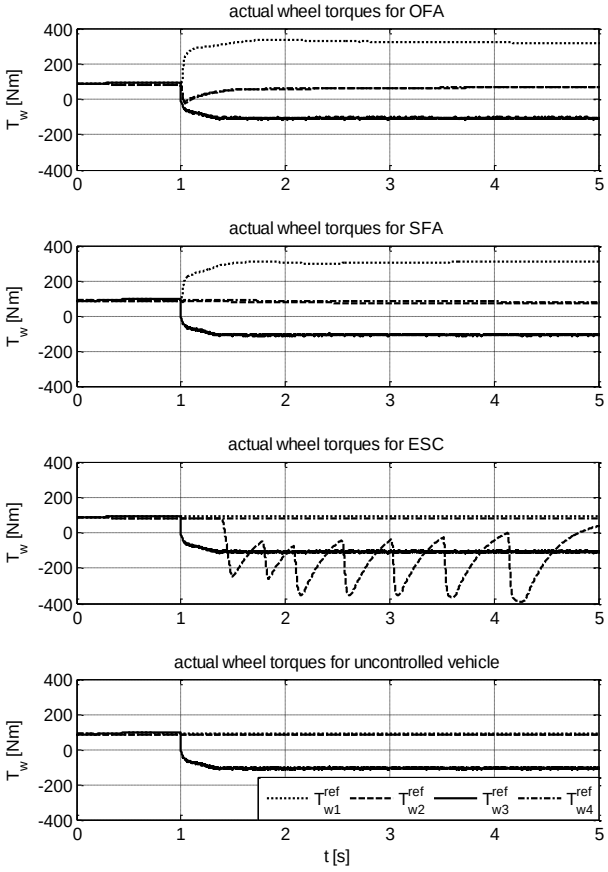

Fig. 8. Torque characteristics during steady-state cornering with an inverter-shutdown at $t = 1$ s.

The results show that for the studied situation, the proposed fault handling strategy tackles faults well in order to preserve vehicle motion and maintain stability during faults. It turns out that the update of the investigated static force allocator from the fault detection and diagnosis function is crucial when major faults occur. Without this function, the vehicle quickly risks to leave the desired trajectory. Exceeding the actuator limitations by reducing the curvature by 10 m only, indicates the operating boundaries of the simplified allocation method. As shown in Fig. 9, the SFA path will move towards the ESC strategy solution when reaching the actuator limits, thus reducing the gains that were made.

For wheel 1, the actual torque reaches its limits shortly after the fault occurs (Fig. 10), while the allocated torque is steadily increasing due to the missing actuator constraints (Fig. 11).

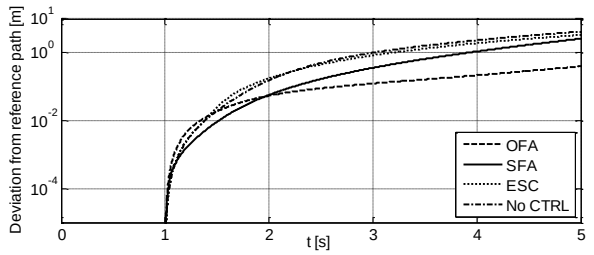

Fig. 9. Overall deviations from reference path for the analysed control strategies at the actuator limit.

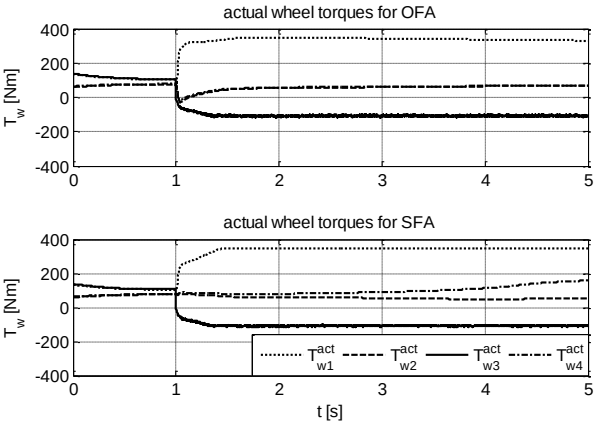

Fig. 10. Torque characteristics at the actuator limit.

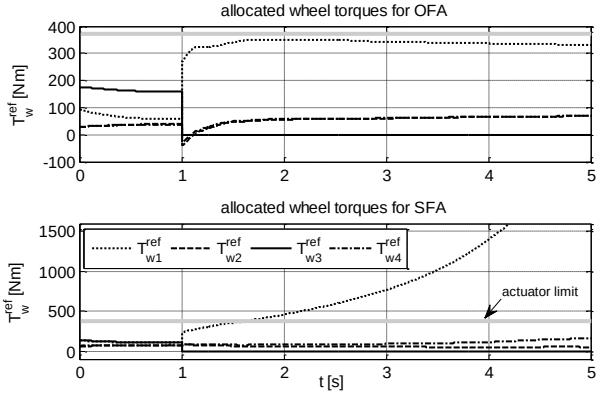

Fig. 11. Allocated torques at the actuator limit.

7. CONCLUSIONS

This study has compared two fault handling strategies based on the force allocation approach. The vehicle behaviour due to the induced fault was investigated and also compared with the behaviour of a reference vehicle. It was shown that the optimised control allocation approach results in the least deviation from the desired path for the studied manoeuvre. The simplified allocation method works well for small in-wheel motor faults as long as the actuator limitations are not reached. It is also shown that the reference vehicle, applying an ESC strategy that uses friction brakes only, is limited to handle this type of electric faults due to slow friction brake force gradients.

ACKNOWLEGDEMENTS

The financial support from SHC Swedish Hybrid Vehicle Centre and TRENoP is gratefully acknowledged.

REFERENCES

[1] Erke, A. “Effects of electronic stability control on accidents: A review of empirical evidence”, Accident Analysis & Prevention, Vol. 40, No. 1, 2008, pp. 167–173.

[2] Wanner, D., Stensson Trigell, A., Drugge, L. and Jerrelind, J. “Survey on fault-tolerant vehicle design”, Proc. of 26th Electric Vehicle Symp., 2012.

[3] Jonasson, M. and Wallmark, O. “Control of electric vehicles with autonomous corner modules: implementation aspects and fault handling”, Vehicle Systems, Modelling and Testing, Vol. 3, No. 3, 2008, pp. 213–228.

[4] Edrén, J., Jerrelind, J., Stensson Trigell, A. and Drugge, L. “Implementation and evaluation of force allocation control of a down scaled prototype vehicle with wheel corner modules”, Submitted 2012.

[5] Knobel, C., Pruckner, A. and Bünte, T. “Optimized force allocation - a general approach to control and to investigate the motion of over-actuated vehicles”, Proc. of 4th IFAC-Symp. on Mechatronic Systems, 2006.

[6] Orend, R. “Steuerung der ebenen Fahrzeug- bewegung mit optimaler Nutzung der Kraftschluss- potentiale aller vier Reifen“, at-Automatisierungstechnik, Vol. 53, No. 1, 2005, pp. 20–27.

[7] Wang, J. and Longoria, R. “Coordinated and reconfigurable vehicle dynamics control”, IEEE Trans. of Control Systems Technology, Vol. 17, No. 3, 2009, pp. 723–732.

[8] Fredriksson, J., Andreasson, J. and Laine, L. “Wheel force distribution for improved handling in a hybrid electric vehicle using nonlinear control”, Proc. of 43rd IEEE Decision and Control, 2004.

[9] ADAC. ADAC Pannenstatistik 2010, www.adac.de. Accessed at 2011-11-17.

[10] Chu, W., Luo, Y., Dai, Y. and Li, K. “Traction fault accommodation system for four wheel independently driven electric vehicle”, Proc. of 26th Electric Vehicle Symp., 2012.

[11] Patton, R. “Fault-tolerant control systems: The 1997 situation”, Proc. of 3rd IFAC Symp. on Fault Detection, Supervision and Safety for Technical Processes, 1997.

[12] Liao, Y. “Analysis of fault conditions in permanent-magnet in-wheel motors”, KTH M.Sc. thesis, 2011.

[13] Isermann, R. “Fehlertolerante mechatronische Systeme I“, at-Automatisierungstechnik, Vol. 55, No. 4, 2007, pp. 70–179.

[14] Jonasson, M., Andreasson, J., Stensson Trigell, A. and Jacobson, B. “Utitilisation of actuators to improve vehicle stability at the limit: from hydraulic brakes towards electric propulsion”, Proc. of IAVSD, 2009.